Femtosecond infrared studies of ligand rearrangement reactions: silyl hydride products from Group 6 carbonyls

K.T. Kotz [a,b], H. Yang [a,b], P.T. Snee [a,b], C.K. Payne [a,b], C.B. Harris [a,b,*]

[a] *Department of Chemistry, University of California, Berkeley, CA 94720, USA*
[b] *Chemical Sciences Division, Ernest Orlando Lawrence Berkeley, National Laboratory, Berkeley, CA 94720, USA*

Accepted 4 November 1999

Abstract

The ultrafast dynamics of the Si–H bond activation reaction by the Group 6 d^6 organometallic compounds $M(CO)_5$ (M = Cr, Mo, and W) have been studied in neat tri-substituted silanes under ambient conditions. The ultrafast spectral evolutions of the CO stretching bands were monitored following UV photolysis using femtosecond pump–probe spectroscopic methods. It was found that the coordinatively unsaturated species, which is formed following CO photolysis from the parent molecule, is quickly solvated (< 2 ps) via the C–H bonds of the solvent. These species then rearranged to the silyl hydride product on a timescale of a few nanoseconds. These results were augmented by rearrangement studies in neat ethanol, propanol and hexanol solutions in which the initially formed metal C–H complex rearranged to the metal hydroxyl complex. The mechanism of this rearrangement was discussed by comparison of the data with various models in the literature. It was found that a mechanism that is primarily dissociative in nature provided the best description of the experimental data. © 2000 Elsevier Science S.A. All rights reserved.

Keywords: IR spectroscopy; Dissociative mechanism; Dynamics; Group 6; Ultrafast spectroscopy

1. Introduction

Hydrosilation is an important synthetic reaction for the generation of substituted silane molecules. Transition-metal complexes are known to catalyze these reactions, often with silyl hydrides postulated as intermediates in this process [1–3]. Recent studies have shown that similar weakly bound complexes between reactive transition-metal complexes and solvent molecules play a role in the product formation of oxidative reactions [4,5]. Group 6 metal carbonyls are known to catalyze the hydrosilation of alkenes [3]. This makes them ideal candidates for studying the processes involved in such chemical reactions. Understanding the solvation and evolution of such silyl hydride intermediates is an important goal towards understanding the general reactivity of hydrosilation transformations.

The detailed photochemistry of Group 6 metal carbonyls is well known [6]. Following irradiation by UV light, the ground-state molecule is promoted into a carbonyl dissociative state. In solution, one CO ligand is lost within 400 fs [7–9]. Surrounding molecules solvate the unsaturated metal fragment within 1–2 ps [10,11]. The metal–CO bond strength of these systems is typically about 35–45 kcal mol^{-1} [12], whereas the UV photons used in photolysis studies typically have ca. 100 kcal mol^{-1}. The excess 55–65 kcal mol^{-1} of energy that the excited unsaturated metal fragments contain is then dissipated to the solvent in tens to hundreds of picoseconds following CO dissociation [13]. The initial solvation of the bare metal fragment happens well before equilibrium of the chemical system has been established. In solutions containing different types of ligands that can bind the unsaturated metal center, the structure of the initial solvation complex that forms is dictated only by the statistical nature of the solvation process, not the thermodynamics of the equilibrated system. This initial kinetic product rearranges to form the thermodynamic product on a timescale dictated by the rearrangement process itself.

Simon and co-workers studied this rearrangement process for the initial coordination of alcohols with photogenerated $Cr(CO)_5$ [10,11,14,15]. In their system, photolysis of $Cr(CO)_6$ in neat alcohols produced pen-

tacarbonyl fragments that coordinated to either the oxygen or the C–H bonds of the alcohol. The weaker alkyl complex rearranged over hundreds of picoseconds to form the more stable O–H bound complex. They proposed an intramolecular chain-walk mechanism to account for the rearrangement dynamics, in which the initial C–H complex rearranges through random walks along the alkyl backbone until the metal center encounters the strongly binding hydroxyl site [15]. This model seems to accurately describe the rearrangement for several alcohols. Their observations, however, were made in the visible region of the spectra where broad linewidths and complicated Frank–Condon overlap factors make it difficult to ascertain the exact structural nature of the reactive intermediates.

This rearrangement process has also been studied by other groups. Using photoacoustic calorimetry (PAC), Burkey determined the bonding enthalpies of $M(CO)_5$ (M = Cr, Mo, and W) with alkanes and silanes [16]. He concluded that the pentacarbonyl–silane complexes are about twice as strong as that of alkane complexes. Dobson and co-workers have studied the process of ligand rearrangement at unsaturated metal centers using PAC and UV–vis flash photolysis techniques [17–26]. These researchers have concluded that the rearrangement of ligands at a $Cr(CO)_5$ center is most likely an intermolecular process, thus raising doubts on the validity of the chain-walk mechanism [24]. However, both the PAC experiments and the flash photolysis studies lacked sufficient time resolution to observe the initial solvation and the subsequent rearrangement process immediately following CO dissociation on the picosecond timescale. With these restrictions, it was not possible to examine the microscopic role of the solvent in such rearrangement processes. It was also beyond the means of these researchers to examine the mechanism of rearrangement when it takes place on a timescale comparable with energy relaxation of the non-equilibrated system.

It is well known that the IR absorbances of metal carbonyls are strongly affected by changes in electronic structure at the transition metal center. Femtosecond time-resolved IR (fs-TRIR) absorption experiments on metal carbonyls have recently appeared in the literature [7,27–38]. The spectroscopic information contained in fs-TRIR spectroscopy allows direct measurement of ultrafast processes with a structurally sensitive probe. With fs-TRIR spectroscopy, processes such as vibrational relaxation and ligand rearrangement can be unambiguously assigned following CO dissociation. Recent experiments carried out by Yang et al. have used ultrafast transient IR pulses to monitor the rearrangement of triethylsilane with the highly reactive 16 e^- transition-metal fragments, $(\eta^5\text{-}C_5H_5)M(CO)_2$ (M = Mn and Re) [31,32]. In these experiments, the manganese and rhenium complexes were photogenerated

from the tricarbonyl species $(\eta^5\text{-}C_5H_5)M(CO)_3$ (M = Mn and Re) and were initially solvated by the ethyl C–H bonds or the silyl Si–H bond in less than 5 ps. The solvated manganese and rhenium dicarbonyls then rearranged from the alkyl solvated species to the stable silane adducts on nanosecond and microsecond timescales, respectively, via an intermolecular dissociative mechanism. Thus, competitive solvation led to different timescales for silyl hydride formation.

We have carried out a series of experiments in order to address the issues related to intermediate formation by highly reactive Group 6 metal carbonyls. We have carefully studied the solvation of highly reactive 16 e^- transition-metal complexes and the formation of metal silyl hydride complexes. We have also studied the rearrangement dynamics for the series of metal carbonyls $M(CO)_6$ (M = Cr, Mo, W) irradiated in triethylsilane. To this end, we have re-examined Simon and co-workers' alcohol solvation experiments, and our results provide new insights into the ligand dynamics for $Cr(CO)_5$. Our data suggest an intermolecular rearrangement of ligands at the coordinatively unsaturated metal centers, confirming the results of Dobson and co-workers [24,26].

2. Experimental

2.1. Sample handling

Metal hexacarbonyls, $M(CO)_6$ (M = Cr, Mo W), were purchased from Pressure Chemicals and were used without further purification. The solvents hexanol (98%), ethanol (anhydrous), and hexanes (98.5% spectrophotometric grade) were purchased from Aldrich. Triethylsilane and tri-*n*-propylsilane were both purchased from Gelest. No differences were observed between experiments carried out in triethylsilane purchased from Gelest and those that were performed in triethylsilane that had been dried over an alumina column and distilled in an inert atmosphere of nitrogen. Furthermore, previous studies of metal hexacarbonyls that were carried out in spectrophotometric grade alkanes purchased from manufacturers showed no signs of contamination due to handling under ambient conditions [7].

The metal carbonyl solutions were prepared with a concentration between 3 and 20 mmol and were placed in a demountable liquid IR flow cell (Harrick Scientific) fitted with CaF_2 windows. The flow-cell thickness and the sample concentration were adjusted in order to optimize the signal arising from the transient species of interest. The samples' purity was assessed regularly using static FTIR, and samples were changed periodically in order to ensure purity.

2.2. Data collection

The femtosecond IR (fs-IR) laser system used in these studies has been previously described in detail [7]. Briefly, the output from a 80 MHz titanium:sapphire oscillator was amplified in two Bethune cell dye amplifiers [39] that were pumped by a 30 Hz Nd:YAG laser (Quanta-Ray GCR). These pulses were split into three lines. The first of these pulses was amplified in one Bethune cell to a final energy of 5 μJ. The other two lines were separately focused into sapphire windows generating a white light continuum. From this white light, wavelengths for final amplification were selected by the appropriate band-pass filters each having a 10 nm full width at half maximum. In these experiments, one pulse was selectively amplified at 590 nm in a three-stage Bethune cell amplifier chain. This pulse was then sent through a variable delay line before being frequency doubled, producing ca. 6 μJ, 200 fs pulses, centered at 295 nm. The second pulse, centered at 690 nm, was similarly amplified to a final energy of 25 μJ. This pulse, along with the 800 nm pulse were difference frequency mixed by focusing into a $LiIO_3$ crystal, producing 80 fs pulses of ca. 1 μJ, tunable between 1800 and 2300 cm^{-1}.

The UV pulses were focused to a ca. 200 μm spot in the sample in order to initiate the chemical reactions. The IR pulses were split into a signal and a reference beam. Subsequent reaction dynamics were monitored by the IR signal pulse. The maximum time delay between the pump pulse and the probe pulse was limited to 700 ps by the length of the translation stage. To make sure that all signals were due to population dynamics, the pump and probe pulse polarizations were set at the magic angle (54.7°) in all of these experiments. Both IR beams were then focused into an astigmatism-corrected spectrographic monochrometer (spectra-Pro-150, Acton Research, 150 gv mm^{-1}, 4.0 μm blazed). The dispersed pulses were projected onto a focal-plane-array (FPA) detector (Talktronics), which consists of a 256×256 element HgCdTe diode array (Ratheon Amber). The frequency-dispersed images were digitized within two separate windows of 12×200 pixels on this diode array, allowing simultaneous normalization of a 170 nm spectrum. The data for two experiments that follow were recorded with an older data-collection scheme [7]. Briefly, the IR pulses were split into a signal and a reference beam. Both the signal beam and the reference beam were then focused into a monochromator and received by a pair of HgCdTe detectors. The time-resolved IR spectra were collected by scanning the monochromator while fixing the time delay between the pump and the probe pulses. The kinetic traces were acquired by setting the monochromator at the desired wavelengths while varying the delay between pump and probe. The typical spectral and temporal resolution for this setup are 4 cm^{-1} and 300 fs, respectively. A broad, frequency independent background signal due to the CaF_2 windows was subtracted from all of the transient spectra.

2.3. Data analysis

The observed spectral changes in the CO stretching region were recorded as difference spectra in which negative bands indicate depletion of parent molecules, while positive bands show the appearance of new chemical species. Repeated measurements were used to obtain errors for the individual spectral points. The spectral points with errors were fit for each individual time slice to a sum of Voight functions by a chi-squared fitting function. The errors for each peak were determined with a Monte Carlo bootstrap fitting procedure in which 200 simulated data sets were used to obtain error estimates [40,41]. The widths of the peaks did not significantly contribute to the dynamics of the integrated peak intensities within the error of the fitting procedure. The peak amplitudes were therefore used in the kinetic analysis of the population dynamics. The spectra at early times ($\Delta t < 14$ ps) could not be accurately fit because the peaks are very broad and featureless. For these early times, the amplitudes centered at later peak positions were used as kinetic points.

The kinetics at each spectral peak were fit to the function

$$A(t) = c_0 + \sum_{i=1}^{N} c_i \exp(-a_i t) \qquad (1)$$

where $A(t)$ is the recorded signal at time delay t and c_i and a_i are constants. The number of exponential functions, N, was determined by the exact kinetic behavior for each individual peak, and will be described later in the text. The fitting function used was again a chi-squared fit using the fitted amplitudes and their associated errors. A numerical simplex algorithm written for MATLAB was used to find the best fits, and the errors associated with the kinetic parameters were calculated based on standard procedures [40,41].

3. Results

3.1. Metal hexacarbonyls in silanes

The spectra for each of the different metal carbonyls, $M(CO)_6$ (M = Cr, Mo, or W), all have similar spectral features. The static IR spectra for the different hexacarbonyls exhibit an intense T_{1u} CO stretching band at 1987, 1989 and 1983 cm^{-1} for chromium, molybdenum and tungsten, respectively. Following UV irradiation, the static FTIR spectra of the individual hexacarbonyls exhibit two new stretching bands red-shifted with re-

spect to the parent T_{1u} band. The two new bands arise from the A and E symmetry CO stretches of the pentacarbonyl silyl hydride complexes that have local

Table 1
Fitted spectral positions

Compound	Ligand [a]	Band	Position (cm^{-1}) [b]
Cr(CO)$_5$L	L = Et–SiHEt$_2$	$E (v = 0 \rightarrow 1)$	1955
		$E (v = 1 \rightarrow 2)$	1945
		$A (v = 0 \rightarrow 1)$	1938
	L = SiHEt$_3$	$E (v = 0 \rightarrow 1)$	1951
		$A (v = 0 \rightarrow 1)$	1947
	L = n-PrSiH(n-Pr)$_2$	$E (v = 0 \rightarrow 1)$	1947
		$A (v = 0 \rightarrow 1)$	1920
	L = SiH(n-Pr)$_3$	$E (v = 0 \rightarrow 1)$	1940
		$A (v = 0 \rightarrow 1)$ [c]	Not resolved
Mo(CO)$_5$L	L = Et–SiHEt$_2$	$E (v = 0 \rightarrow 1)$	1963
		$E (v = 1 \rightarrow 2)$	1947
		$A (v = 0 \rightarrow 1)$	1925
	L = SiHEt$_3$	$E (v = 0 \rightarrow 1)$	1956
		$A (v = 0 \rightarrow 1)$	1934
W(CO)$_5$L	L = Et–SiHEt$_2$	$E (v = 0 \rightarrow 1)$	1953
		$E (v = 1 \rightarrow 2)$	1945
		$A (v = 0 \rightarrow 1)$	1935
	L = SiHEt$_3$	$E (v = 0 \rightarrow 1)$	1950
		$A (v = 0 \rightarrow 1)$ [c]	Not resolved

[a] Complexation to the unsaturated metal center occurs through the functional group at the beginning of the ligand description.
[b] Uncertainties of ± 2 cm^{-1}.
[c] The alkyl and silyl bands could not be resolved for this peak.
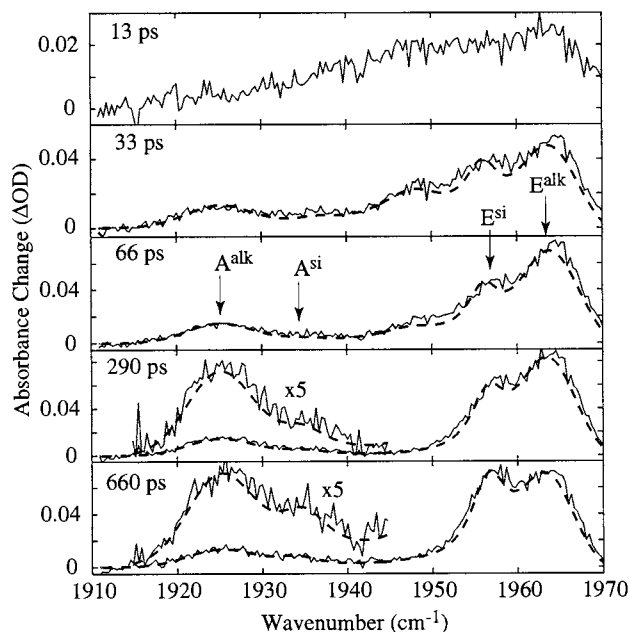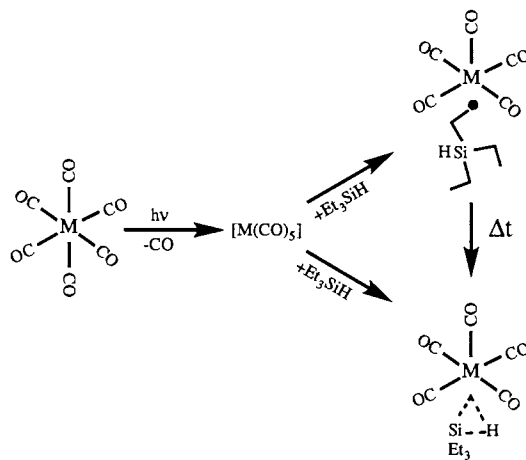

Fig. 1. Transient difference spectra in the CO stretching region for Mo(CO)$_6$ in neat triethylsilane at 13, 33, 66, 290 and 660 ps following 295 nm UV photolysis. The A and E CO stretching bands of the alkyl solvate or silyl adduct of Mo(CO)$_5$ are labeled. The fit to the data appears as a dashed line.

Scheme 1. Reaction sequence.

C_{4v} symmetry at the metal center. The peak positions of these peaks can be found in Table 1 and will be discussed below. The fs-TRIR transient absorption spectra following UV excitation for Mo(CO)$_6$ in triethylsilane are shown in Fig. 1. These spectra contain features that are present in all of the metal carbonyl systems studied in this paper and will be used as a representative example of the time-resolved spectral behavior of these systems [42].

There are five salient features which appear in the individual spectra of Fig. 1. The presence of each of these features can be attributed to the different pentacarbonyl molecules shown in Scheme 1. These pentacarbonyl fragments have approximate C_{4v} symmetry and exhibit two carbonyl stretching bands of A and E symmetry, respectively. Because the silicon–hydrogen bond is a better electron donor than the carbon–hydrogen bond, the E and A bands of the silyl complex typically appear frequency shifted with respect to those of the alkyl complex. In the ultrafast spectra of Fig. 1, the alkyl and silyl E bands, labeled E^{alk} and E^{sil}, respectively, are more intense and appear to the blue of the alkyl and silyl A bands, labeled A^{alk} and A^{sil}. The silyl E band appears as a shoulder on the red edge of the alkyl E band, whereas the silyl A band appears on the blue edge of the alkyl A band. There is also a feature that appears between the E and the A bands at early time delays between pump and probe. This feature decays away within 100 ps. It is assigned to the hot-band transition $v = 1 \rightarrow 2$ of the alkyl E band. Two of the systems studied exhibited slight deviations from spectral behavior observed in the molybdenum spectra of Fig. 1. In the case of tungsten hexacarbonyl dissolved in triethylsilane, the silyl A and alkyl A bands could not be resolved from one another. This was also true for the A bands of Cr(CO)$_5$ in tri-n-propylsilane.

The fitted peak positions and peak assignments for the features that appear in the different fs-TRIR transient spectra are compiled in Table 1. The assignments for the M(CO)$_5$ (M = Cr, Mo, W) silyl *E* bands are based on literature values for similar silyl complexes [16]. The alkyl band assignments, including the hot-band assignments, for all of the metal systems are found to agree with values reported in the literature for pentacarbonyls generated in neat alkanes [36]. The assignments for the silyl *A* bands of the pentacarbonyl complexes are based on analogy to the *A* alkyl bands.

The amplitudes for each of the spectral peaks in Table 1 were fitted to Eq. (1). The kinetic behavior of the individual peaks showed remarkable similarity amongst the different metal systems. The alkyl *A* and *E* bands for each of the metals were fit to a single growth on the picosecond timescale followed by a decay on the nanosecond timescale. The alkyl *E* hot bands were fit to a fast growth followed by a fast decay, both on the picosecond timescale. The numbers obtained from this latter decay, as well as the numbers obtained from the growth of the *A* and *E* bands were consistent with vibrational relaxation times for these systems [36,43]. The silyl *E* bands exhibited bi-exponential growth. The first component was on the picosecond timescale, and again was indicative of fast vibrational relaxation. The second component was on the nanosecond timescale. A summary of the fitted parameter values can be found in Table 2.

The kinetics for the Mo(CO)$_5$ alkyl and silyl *E* bands appear in Fig. 2. The alkyl *A* band exhibits an initial fast rise of 44 ps followed by a 1.6 ns decay. The silyl *E* band exhibits an initial rise of 22 ps, which is followed by a longer growth component of 2 ns. The similarity between the slow decay of alkyl band and the slow growth of the silyl band shows that these species are kinetically linked. This kinetic link is seen for all of the hexacarbonyl systems studied in this paper and reflects the interconversion between the alkyl and silyl complexes, on a nanosecond timescale. The kinetic traces for the chromium and tungsten complexes are similar to the molybdenum kinetics and can be obtained from the authors. Shown in Fig. 3 are the alkyl *E* band kinetics for Cr(CO)$_6$ dissolved in triethylsilane and tri-*n*-propylsilane. As can be seen in the Figure, the two peaks decay with ca. the same rate.

The kinetics for the silyl *A* bands in the molybdenum and chromium systems exhibit interesting behavior. The kinetics for the silyl *A* band show an initial decay of ca. 15 ps, followed by a growth of ca. 4 ns. Because the early time spectra are very broad, the kinetic data at early times (< 20 ps) cannot be resolved into peaks. This broadening has been attributed to overlap with excited lower-frequency vibrational modes of the molecule and to a harmonic coupling to other intramolecular vibrational modes [36,44]. It is possible

that nearby bands are broadened and become overlapped with the *A* band. The initial decay can therefore be attributed to the narrowing of these nearby peaks. The timescale for this initial decay would then describe cooling of the low-frequency modes coupled to or overlapped with this carbonyl stretch. It is also possible that a separate band with the same frequency as the silyl *A* band is contributing to the initial decay. For the molybdenum pentacarbonyl, the alkyl *E* band has a hot band 16 cm^{-1} red-shifted from the ground state vibrational transition. The silyl *A* band is red-shifted 22 cm^{-1} from the silyl *E* band. It may be possible that the silyl *E* band $v = 1 \rightarrow 2$ transition overlaps with the silyl *A* band. The decay of 15 ps could then be attributed to the vibrational cooling of the *E* $v = 1 \rightarrow 2$ transition, and would be consistent with the cooling time for the alkyl adduct bands mentioned above. Neither explanation can be ruled out given the signal to noise ratio of our data in this region. Regardless of the nature of the origin of this decay component, we believe that it is due to a process separate from the formation of the silyl *A* band. The data for the chromium silyl *A* band can be explained in a similar manner. The fit parameters described above also appear in Table 2.

3.2. Cr(CO)$_6$ in alcohols

The femtosecond dynamics following UV irradiation were recorded for Cr(CO)$_6$ dissolved in ethanol, 1-propanol, 2-propanol and 1-hexanol. There are four discernable features in the fs-TRIR spectra for Cr(CO)$_6$ in 1-hexanol, shown in Fig. 4. The first is the parent bleach at 1985 cm^{-1}. The next feature is the peak at 1959 cm^{-1}, attributed to the complex between the pentacarbonyl fragment and the C–H bonds of the alcohol. This assignment was based on the peak position relative to the parent complex, and the peak position of the alkyl *E* band in alkane solution. The alkyl *A* band, expected to appear near 1940 cm^{-1} was not observed because of the rather large intensity of the hydroxyl *E* band that appears in this region of the spectra. The peaks at 1896 and 1940 cm^{-1}, which can be observed in the static FTIR spectra, were due to the *A* and *E* bands, respectively, of the long-lived hydroxyl-bound complex. In 1-hexanol the alkyl complex rearranged to the thermodynamically more stable hydroxyl complex on a timescale of 1.8 ns.

Fig. 5 shows the fs-TRIR spectra for Cr(CO)$_6$ in 2-propanol solution. The features in these spectra are the same as those in 1-hexanol. The spectra for the 1-propanol are nearly identical to those in 2-propanol and can be obtained from the authors. The main difference between the propanol data and the hexanol data is the timescale for rearrangement between the alkyl and hydroxyl complexes. It is clear that this rearrangement in propanol occurs well before the final spectral trace of

660 ps. The rearrangement from alkyl to hydroxyl complexes occurs with time constants of 160 ± 90 ps in 1-propanol and 100 ± 40 ps in 2-propanol. Fig. 6 shows the fs-TRIR spectra of $Cr(CO)_6$ in ethanol. Unlike the propanol and hexanol data, the alkyl complex is not observed. This will be discussed later in the text. The formation of the hydroxyl complex occurs with a time constant of ca. 200 ps.

4. Discussion

4.1. Metal carbonyl kinetics

The kinetics for each of the spectral features amongst the different metal systems are remarkably similar. As mentioned above, the kinetics suggest rearrangement from the alkyl complex to the silyl complex. The trend in rearrangement timescales follows the order $Mo < Cr < W$. This trend is consistent with the observed dissociation enthalpies of various alkanes from $M(CO)_5$ ($M = Cr, Mo, W$) [12]. As discussed above, the ultrafast spectra for the different alkyl complexes are spectroscopically similar to those in alkane solution. This suggests that the alkyl chains of silanes behave much like free alkane molecules. This has also been observed in previous silane studies [31]. The overall similarity in
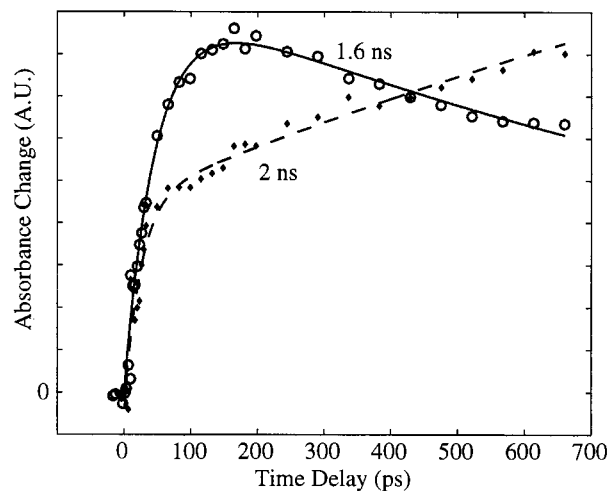

Fig. 2. Ultrafast kinetics of $Mo(CO)_5$ in neat triethylsilane after 295 nm UV photolysis observed at: 1963 cm^{-1}, the CO stretch of the alkyl solvate $Mo(CO)_5$ E band (open circles); 1956 cm^{-1}, the CO stretch of the silyl adduct $Mo(CO)_5$ E band (closed diamonds). The time constants for the exponential fits (smooth curves) are shown in the graph.

bond energetics, and similar kinetic rates for the rearrangement process strongly suggests a similar mechanism for rearrangement from the alkyl to the silyl solvate for the different metal systems.

Table 2
Kinetic parameters for fits to Eq. (1) [a]

Metal carbonyl	Ligand [b]	Band	Kinetic description [c]	Fast component lifetime (ps)	Slow component lifetime (ns)
$Cr(CO)_5L$	$L = Et–SiHEt_2$	E ($v = 0 \to 1$)	Rise/decay	19 ± 2	4 ± 1
		E ($v = 1 \to 2$)	Rise/decay [d]		
		A ($v = 0 \to 1$)	Rise/decay	19 ± 2	2.3 ± 0.8
	$L = SiHEt_3$	E ($v = 0 \to 1$)	Growth	<5 [d]	2.3 ± 10
		A ($v = 0 \to 1$)	Decay/growth	15 ± 3	4.3 ± 27
	$L = n\text{-}PrSiH(n\text{-}Pr)_2$	E ($v = 0 \to 1$)	Rise/decay	45 ± 5	2.4 ± 5
		A ($v = 0 \to 1$)	Rise/decay	50 ± 30	2.4 ± 1.1
	$L = SiH(n\text{-}Pr)_3$	E ($v = 0 \to 1$)	Growth	60 ± 12	3 ± 11
		A ($v = 0 \to 1$)	Not resolved		
$Mo(CO)_5L$	$L = Et–SiHEt_2$	E ($v = 0 \to 1$)	Rise/decay	44 ± 8	1.6 ± 0.3
		E ($v = 1 \to 2$)	Rise/decay	15.6 ± 1.3	0.0296 ± 0.0012
		A ($v = 0 \to 1$)	Decay	38 ± 7	1.9 ± 1.4
	$L = SiHEt_3$	E ($v = 0 \to 1$)	Growth	22 ± 2	2 ± 7
		A ($v = 0 \to 1$)	Growth	15 ± 17	2 ± 17
$W(CO)_5L$	$L = Et–SiHEt_2$	E ($v = 0 \to 1$)	Decay	48 ± 5	2.4 ± 0.4
		E ($v = 1 \to 2$)	Decay	<5 [d]	0.039 ± 0.001
		A ($v = 0 \to 1$)	Decay	40 ± 20	4 ± 3
	$L = SiHEt_3$	E ($v = 0 \to 1$)	Growth	22 ± 16	2 ± 5
		A ($v = 0 \to 1$)	Not resolved		

[a] Errors represent one S.D.

[b] Complexation to the unsaturated metal center occurs through the functional group at the beginning of the ligand description.

[c] Rise/decay were fitted to Eq. (1) with $N = 2$, $c_1 < 0$, $c_2 > 0$; growth was fit to Eq. (1) with $N = 2$, $c_1 < 0$, $c_2 < 0$, $c_0 > 0$; decay/growth were fitted to Eq. (1) with $N = 2$, $c_1 > 0$, $c_2 < 0$, $c_0 > 0$.
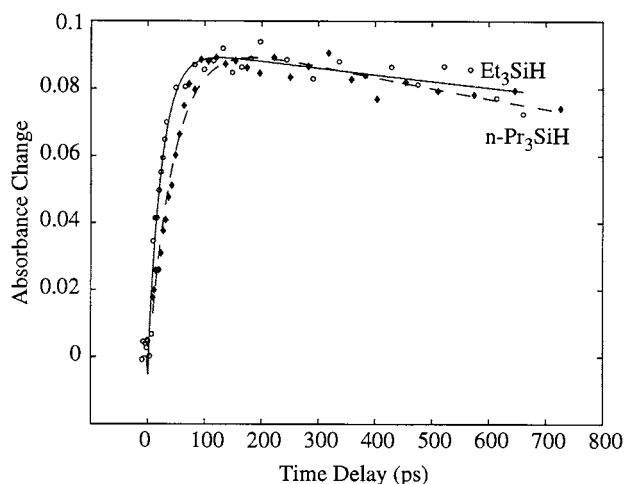
[d] These components could not accurately be fitted.

Fig. 3. Comparison of the ultrafast kinetics of the alkyl solvate $Cr(CO)_5$ in neat triethylsilane and in neat tri-*n*-propylsilane after 295 nm UV photolysis observed at: the CO stretch of the alkyl solvate $Cr(CO)_5$ *E* band in triethylsilane (open circles); the CO stretch of the alkyl solvate $Cr(CO)_5$ *E* band in tri-*n*-propylsilane $Cr(CO)_5$ (closed diamonds).

4.2. The chain-walk mechanism

The ultrafast rearrangement of alcohols with $Cr(CO)_5$ metal centers was previously studied by Simon and co-workers using picosecond UV–vis spectroscopy [10,11,14,15,45]. They modeled the rearrangement as an intramolecular process by which a bound solvent molecule would change its coordination to the unsaturated metal center by walking along the backbone of the carbon chain [15]. Their model included only two parameters: (1) k_{cc}, the rate at which the molecule walked between methylene units of the alcohol backbone; and (2) k_{co}, the rate for walking onto the strong-binding hydroxyl site. They proposed the chain-walk mechanism to describe the rearrangement at alcohols based on the observation that the rearrangement time for 1-propanol was ca. 200 ps, whereas the rearrangement time in 2-propanol was identical to the rearrangement time in ethanol, ca. 80 ps. They found that a single pair of rate constants (k_{cc} and k_{co}) was able to fit the kinetic data for a series of linear alcohols with 2–8 carbons in the alkyl chain. Ultrafast studies in the UV–vis range, however, can be obscured by the very complex potential energy surface of large molecules, and the visible probe used in such studies probes the Frank–Condon overlap between the ground-state and complicated excited-state electronic potential energy surfaces.

Our fs-TRIR results probe the actual populations of both the hydroxyl and silyl adducts. Because metal–carbonyl stretching frequencies are strongly affected by the electronic density at the metal center, both of these adducts can be unambiguously identified with IR spec-

troscopy. From our observations, it seems clear that there is only a slight difference between the rearrangement times of 1-propanol and 2-propanol. Furthermore, the rearrangement times for 1-propanol, 2-propanol, and ethanol are all the same within the error of the measurements. The differences in rearrangement times between these solvents observed by Simon and co-workers probably arose from changes in the Frank–Condon overlap due to vibrational cooling in the ground-state wells of the alkyl and hydroxyl complexes. Our IR data seems to call into question the fundamental experimental basis for the chain-walk mechanism.

The chain-walk mechanism also fails to accurately describe the silane data. The adaptation of the chain-walk mechanism to the silane rearrangement studies is depicted in Scheme 2. If we try to use the chain-walk mechanism to describe the silane data, qualitatively, we see that the rearrangement time in triethylsilane should be similar to the rearrangement time for ethanol. Both involve a single walk from the weakly bound sites to the stronger of the binding sites of the solvent. The main differences between the two solvents would appear as different initial coordination statistics, and dif-
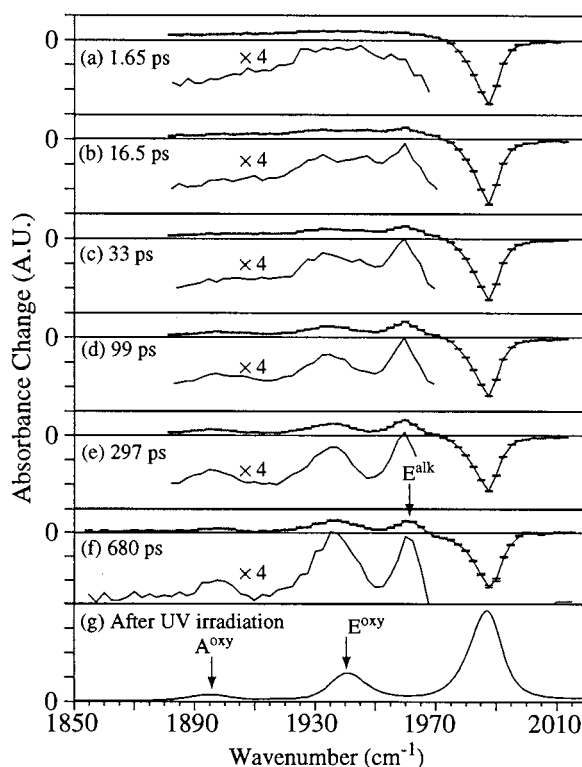

Fig. 4. Transient difference spectra in the CO stretching region for $Cr(CO)_6$ in neat 1-hexanol at 1.65, 16.5, 33, 99, 297, 680 ps and the static difference spectra following 295 nm UV photolysis. The *A* and *E* CO stretching bands of the alkyl solvate or the OH adduct of $Cr(CO)_5$ are labeled. These data were taken using single-element MCT detectors, described in the Section 2.
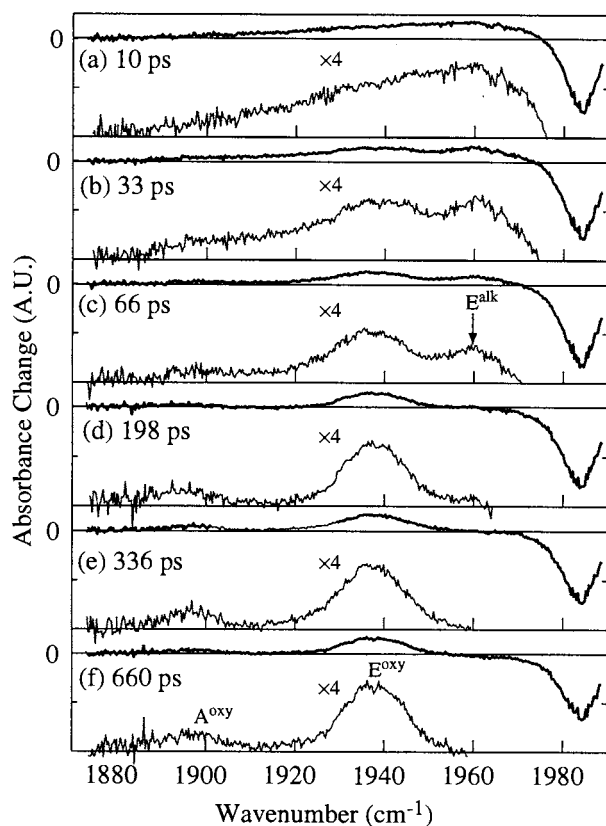
Fig. 5. Transient difference spectra in the CO stretching region for $Cr(CO)_6$ in neat 2-propanol at 10, 33, 66, 198, 336 and 660 ps following 295 nm UV photolysis. The A and E CO stretching bands of the alkyl solvate or the OH adduct of $Cr(CO)_5$ are labeled.

ferences in the rates for walking onto the strongly bound sites. Our data show that the rearrangement in triethylsilane is at least 20 times slower than in ethanol. One could argue that the rate for walking onto a hydroxyl site could be less than the rate to form a Si–H complex due to increased steric hindrance at the Si–H site as compared to the hydroxyl site. It could also be the case that the hydroxyl 'hop' is facilitated by some sort of transition-state stabilization by the hydroxyl moiety. In order to test the generality of the chain-walk, we conducted an experiment in a silane with longer alkyl chains substituted at the silicon atom. Based on the chain-walk mechanism, we would expect the alkyl complex in such a silane to rearrange at a noticeably slower rate when compared to triethylsilane. However, our observations seem to indicate that the alkyl solvate rearrangement times are approximately the same for either $n\text{-}Pr_3SiH$ or triethylsilane silane solvent. The chain-walk mechanism, therefore, seems to be unable to describe the rearrangement of silanes in chromium carbonyl complexes. These observations for rearrangement in silanes and alcohols lead us to conclude that the strictly intramolecular chain-walk mechanism proposed by Simon and co-workers fails to

describe the rearrangement of ligands at Group 6, unsaturated transition metal complexes.

4.3. Rearrangement dynamics

The mechanism describing ligand rearrangement at unsaturated metal centers has been thoroughly studied by Dobson's group. They proposed that the mechanism for rearrangement resembled the process shown in Scheme 3(A), where M is chromium, L_w is a weakly binding token ligand, and L_s is a strongly binding electron-donating ligand [24,26]. This mechanism was found to fit their data for a large variety of ligands, L_w
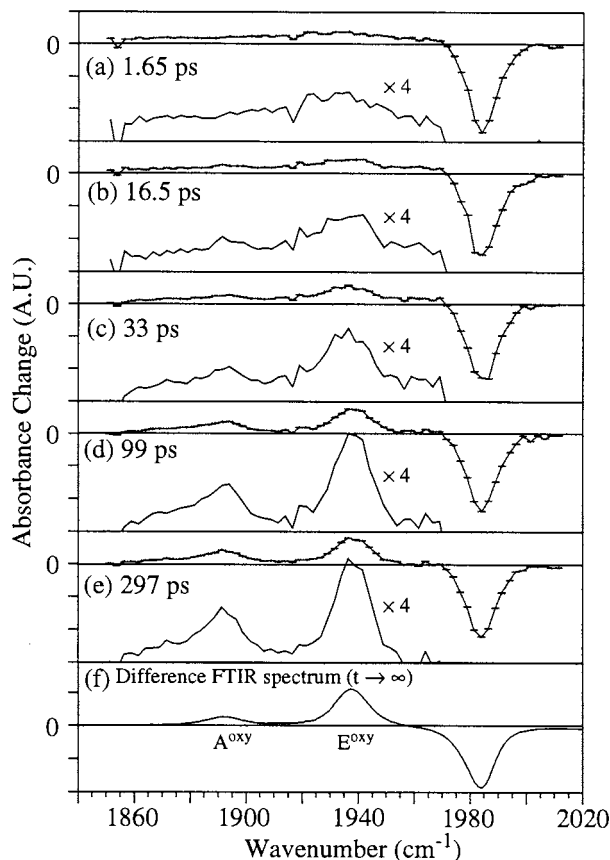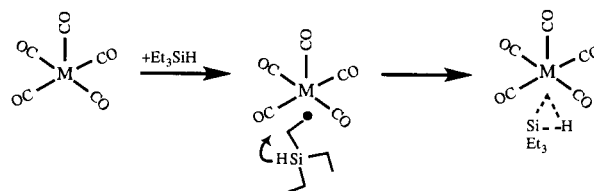

Fig. 6. Transient difference spectra in the CO stretching region for $Cr(CO)_6$ in neat ethanol at 1.65, 16.5, 33, 99, 297 ps and the static difference spectra following 295 nm UV photolysis. The A band of the OH adduct $Cr(CO)_5$ and E band of the alkyl solvate $Cr(CO)_5$ are labeled. These data were taken using single-element MCT detectors, described in the Section 2.
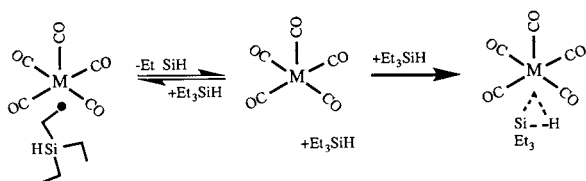

Scheme 2. Chain-walk mechanism.

A. Dobson Mechanism:
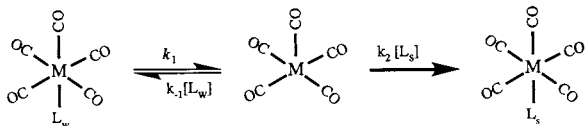
B. Silane Rearrangement:

Scheme 3. Dissociative rearrangement.

and L_s. As was previously mentioned, these experiments lacked the time resolution to rule out the possibility of chain-walk, especially for weakly bound ligands such as short chain alkanes. In light of the above discussion, it seems unlikely that chain-walk occurs in solution for the Group 6 metal complexes. The mechanism proposed by Dobson and co-workers seems to describe accurately the ligand dynamics for chemical systems in this study. This mechanism adapted to the silane studies is shown in Scheme 3(B), where L_w has been changed to the ethyl ligand on the silane and L_s has become the silicon–hydrogen bond of the silane. Because the bare metal fragments are known to solvate extremely rapidly (ca. 1–2 ps), the rates k_{-1} and k_2 in Dobson's mechanism are expected to be extremely fast. The overall mechanism should therefore be limited by the dissociation rate of the L_w ligand, k_1. It is interesting to note that the rearrangement from an alkyl to a silyl complex for the Group 7 complexes (η^5-C_5H_5)M(CO)$_2$ (M = Mn and Re) was also described as being dissociative in nature [32,46,47]. In these latter systems, rearrangement times were orders of magnitude greater than those for the Group 6 systems. These differences can be attributed to the differences in binding enthalpies for the alkyl complexes between the Group 6 and Group 7 complexes [16,48–50]. Preliminary experiments also seem to indicate that rearrangement of the alkyl solvate at the 16 e$^-$ chromium metal center of (η^6-C_6H_6)Cr(CO)$_3$ occurs with a barrier similar to that for the hexacarbonyl complexes, ca. 5.6–6.0 kcal mol^{-1} [51]. We were able to deduce an approximate timescale of 4 ns for the rearrangement process of this half-sandwich complex. These observations, along with the data presented earlier, suggests the dissociative mechanism in Scheme 2 is somewhat general for the rearrangement of ligands at a variety of transition metal centers.

The interaction between the metal pentacarbonyls M(CO)$_5$ (M = Cr, Mo, and W) and the alkyl carbon–hydrogen bond is known to be weak (ca. 7–9 kcal

mol^{-1}) [16,52–54]. With such small complexation energies comparable to that of solvent–solute interactions, it is expected that the potential of mean force should be largely affected. This results in the observed free-energy barriers (5.5–6 kcal mol^{-1}) for the rearrangement process that are lower than the complexation energies (ca. 7–9 kcal mol^{-1}). This barrier lowering can be attributed to the influence of the solvent molecules on the reaction pathway. One possible scenario describing this effect is the involvement of an additional solvent molecule in an associative manner in which the extra solvent molecule is contained in the transition state. The dynamic origin of this barrier lowering is not clear at the microscopic level, but it is expected that the microscopic details of the solvation process contribute to the energetics of the rearrangement processes.

The data for photogenerated Cr(CO)$_5$ in ethanol gives some insight into the complex nature of the microscopic solvation process. The absence of the alkyl peaks in the Cr(CO)$_5$–EtOH data indicates that the Cr(CO)$_5$ fragment is preferentially solvated to the hydroxyl end of the ethanol. This suggests that that the initial solvation following CO dissociation is non-statistical in behavior. This could be due to a number of factors including the size of the solvent or the hydrogen bonding properties of ethanol. In any case, it is clear that the initial solvation is different in ethanol than it is in other alcohols. We are currently studying the nature of this solvation in greater detail. We believe that the details from such studies are relevant to understanding the observed reactivity of these transition metal complexes and that these microscopic details of solvation may give greater insight into the transition state discussed above.

5. Conclusions

To the best of our knowledge, this paper represents the first study that has simultaneously resolved both the spectral components and the detailed ultrafast spectral evolution of the CO stretching bands of the alkyl and silyl complexes following CO dissociation of the parent hexacarbonyl molecules M(CO)$_6$ (M = Cr, Mo, W) in silane solution.

A number of trends were observed for the reactivity of photogenerated Group 6 metal pentacarbonyls. The rearrangement of ligands at these coordinately unsaturated metal centers occurs through a previously proposed mechanism [24,26]. The rate for this rearrangement decreases as the ligand binding enthalpy of the alkyl intermediates increases. Furthermore, the previously reported intramolecular chain-walk mechanism does not accurately describe the rearrangement process in the chemical systems reported in this paper [15]. Further studies are necessary to test the generality

of the dissociative-type mechanism for the reaction of different ligands with transition metal complexes. In particular, it is important to understand the effects of steric hindrance on the rearrangement process, which we believe may have an influential role in the catalytic reactivity of organometallics.

Acknowledgements

References

[1] W. Jetz, W.A.G. Graham, Inorg. Chem. 10 (1970) 4.
[2] M. Wrighton, M.A. Schroeder, J. Am. Chem. Soc. 95 (1973) 5764.
[3] M. Wrighton, M.A. Schroeder, J. Am. Chem. Soc. 96 (1974) 6235.
[4] S.E. Bromberg, H. Yang, M.C. Asplund, T. Lian, B.K. McNamara, K.T. Kotz, J.S. Yeston, M. Wilkens, H. Frei, R.G. Bergman, C.B. Harris, Science 278 (1997) 260.
[5] B.A. Arndtsen, R.G. Bergman, T.A. Mobley, T.H. Peterson, Acc. Chem. Res. 28 (1995) 154.
[6] G.L. Geoffroy, M.S. Wrighton, Organometallic Photochemistry, Academic Press, New York, NY, 1979.
[7] T.Q. Lian, S.E. Bromberg, M.C. Asplund, H. Yang, C.B. Harris, J. Phys. Chem. 100 (1996) 11994.
[8] A.G. Joly, K.A. Nelson, Chem. Phys. 152 (1991) 69.
[9] A.G. Joly, K.A. Nelson, J. Phys. Chem. 93 (1989) 2876.
[10] J.D. Simon, X. Xie, J. Phys. Chem. 91 (1987) 5538.
[11] J.D. Simon, X. Xie, J. Phys. Chem. 90 (1986) 6751.
[12] J.M. Morse, G.H. Parker, T.J. Burkey, Organometallics 8 (1989) 2471.
[13] S.-C. Yu, X. Xu, R. Lingle, J.B. Hopkins, J. Am. Chem. Soc. 112 (1990) 3668.
[14] X. Xie, J.D. Simon, J. Am. Chem. Soc. 93 (1989) 291.
[15] X. Xie, J.D. Simon, J. Am. Chem. Soc. 112 (1990) 1130.
[16] T.J. Burkey, J. Am. Chem. Soc. 112 (1990) 8329.
[17] S. Zhang, G.R. Dobson, T.L. Brown, J. Am. Chem. Soc. 113 (1991) 6908.
[18] S.L. Zhang, V. Zang, H.C. Bajaj, G.R. Dobson, R. Vaneldik, J. Organomet. Chem. 397 (1990) 279.
[19] S. Zhang, G.R. Dobson, Inorg. Chim. Acta 165 (1989) 11.
[20] S.L. Zhang, G.R. Dobson, Inorg. Chim. Acta 181 (1991) 103.
[21] S. Zhang, H.C. Bajaj, V. Zang, G.R. Dobson, R. Vaneldik, Organometallics 11 (1992) 3901.
[22] S.L. Zhang, G.R. Dobson, Organometallics 11 (1992) 2447.
[23] S. Ladogana, S.K. Nayak, J.P. Smit, G.R. Dobson, Inorg. Chim. Acta 267 (1998) 49.
[24] S. Ladogana, S.K. Nayak, J.P. Smit, G.R. Dobson, Inorg. Chem. 36 (1997) 650.
[25] G.R. Dobson, K.J. Asali, C.D. Cate, C.W. Cate, Inorg. Chem. 30 (1991) 4471.
[26] G.R. Dobson, S.L. Zhang, J. Coord. Chem. 47 (1999) 409.
[27] K.D. Rector, A.S. Kwok, C. Ferrante, A. Tokmakoff, C.W. Rella, M.D. Fayer, J. Chem. Phys. 106 (1997) 10027.
[28] D.J. Myers, R.S. Urdahl, B.J. Cherayil, M.D. Fayer, J. Chem. Phys. 107 (1997) 9741.
[29] J.B. Asbury, H.N. Ghosh, J.S. Yeston, R.G. Bergman, T.Q. Lian, Organometallics 17 (1998) 3417.
[30] T. Lian, S.E. Bromberg, H. Yang, G. Proulx, R.G. Bergman, C.B. Harris, J. Am. Chem. Soc. 118 (1996) 3769.
[31] H. Yang, K.T. Kotz, M.C. Asplund, C.B. Harris, J. Am. Chem. Soc. 119 (1997) 9564.
[32] H. Yang, M.C. Asplund, K.T. Kotz, M.J. Wilkens, H. Frei, C.B. Harris, J. Am. Chem. Soc. 120 (1998) 10154.
[33] H. Yang, K.T. Kotz, M.C. Asplund, M.J. Wilkens, C.B. Harris, Acc. Chem. Res. 32 (1999) 551.
[34] M.W. George, T.P. Dougherty, E.J. Heilweil, J. Phys. Chem. 100 (1996) 201.
[35] W.T. Grubbs, T.P. Dougherty, E.J. Heilweil, Chem. Phys. Lett. 227 (1994) 480.
[36] T.P. Dougherty, E.J. Heilweil, Chem. Phys. Lett. 227 (1994) 19.
[37] T.P. Dougherty, W.T. Grubbs, E.J. Heilweil, J. Phys. Chem. 98 (1994) 9396.
[38] T.P. Dougherty, E.J. Heilweil, J. Chem. Phys. 100 (1994) 4006.
[39] D.S. Bethune, Appl. Opt. 20 (1981) 1987.
[40] Y. Bard, Nonlinear Parameter Estimation, Academic Press, Orlando, FL, 1974.
[41] W.H. Press, S.A. Teukolsky, W.T. Vetterling, B.P. Flannery, Numerical Recipies in C, 2nd edition, Cambridge University Press, New York, NY, 1994.
[42] The fs-TRIR spectra for W(CO)$_6$ in triethylsilane and for Cr(CO)$_6$ in triethylsilane or tri-*n*-propylsilane can be obtained from the authors upon request.
[43] S.M. Arrivo, T.P. Dougherty, W.T. Grubbs, E.J. Heilweil, Chem. Phys. Lett. 235 (1995) 247.
[44] P. Hamm, S.M. Ohline, W. Zinth, J. Chem. Phys. 106 (1997) 519.
[45] J.D. Simon, K.S. Peters, Chem. Phys. Lett. 98 (1983) 53.
[46] R.H. Hill, M.S. Wrighton, Organometallics 6 (1987) 632.
[47] R.H. Hill, B.J. Palmer, Organometallics 8 (1989) 1651.
[48] P.-F. Yang, G.K. Yang, J. Am. Chem. Soc. 114 (1992) 6937.
[49] X.Z. Sun, D.C. Grills, S.M. Nikiforov, M. Poliakoff, M.W. George, J. Am. Chem. Soc. 119 (1997) 7521.
[50] J.K. Klassen, M. Selke, A.A. Sorensen, G.K. Yang, J. Am. Chem. Soc. 112 (1990) 1267.
[51] Unpublished results. Data can be obtained from the authors upon request.
[52] S. Zaric, M.B. Hall, J. Phys. Chem. A 101 (1997) 4646.
[53] G.K. Yang, V. Vaida, K.S. Peters, Polyhedron 7 (1988) 1619.
[54] K.E. Lewis, D.M. Golden, G.P. Smith, J. Am. Chem. Soc. 106 (1984) 3905.